

HEPHY-PUB 771/03
hep-ph/0305250

Improved full one-loop corrections to $A^0 \rightarrow \tilde{q}_1 \bar{\tilde{q}}_2$ and $\tilde{q}_2 \rightarrow \tilde{q}_1 A^0$

C. Weber, H. Eberl, W. Majerotto

*Institut für Hochenergiephysik der Österreichischen Akademie der Wissenschaften,
A-1050 Vienna, Austria*

Abstract

We calculate the full electroweak one-loop corrections to the decay of the CP-odd Higgs boson A^0 into scalar quarks in the minimal supersymmetric extension of the Standard Model (MSSM). Due to the complex structure of the electroweak sector a proper renormalization of many parameters in the on-shell renormalization scheme is necessary. For the decay into sbottom quarks, especially for large $\tan \beta$, the corrections can be very large in the on-shell renormalization scheme, which makes the perturbation series unreliable. We solve this problem by an appropriate definition of the tree-level coupling in terms of running quark masses and running trilinear couplings A_q . We also discuss the decay of heavy scalar quarks into light scalar quarks and A^0 . We find that the corrections are significant and therefore cannot be neglected.

1 Introduction

The Minimal Supersymmetric Standard Model (MSSM) [1] requires five physical Higgs bosons: two neutral CP–even (h^0 and H^0), one heavy neutral CP–odd (A^0), and two charged ones (H^\pm) [2, 3]. The existence of a CP–odd neutral Higgs boson would provide a conclusive evidence of physics beyond the SM. Searching for Higgs bosons is one of the main goals of present and future collider experiments at TEVATRON, LHC or an e^+e^- Linear Collider.

In this paper, we consider the decay of the CP–odd Higgs boson A^0 into two scalar quarks, $A^0 \rightarrow \tilde{q}_1 \tilde{q}_2$. The decays into squarks can be the dominant decay modes of Higgs bosons in a large parameter region if the squarks are relatively light [4, 5]. In particular, the third generation squarks \tilde{t}_i and \tilde{b}_i can be much lighter than the other squarks due to their large Yukawa couplings and their large left–right mixing. We will calculate the *full* electroweak corrections in the on–shell scheme and will implement the SUSY–QCD corrections which were calculated previously [6]. The challenge of this calculation is the necessity to renormalize almost all parameters in the electroweak sector in only one single process. Due to the numerous electroweak interacting particles and the complex coupling structure we have to compute a large number of graphs. In general, the Higgs–squark–squark couplings consist of F – and D –terms and SUSY breaking terms, all depending on the squark mixing angle $\theta_{\tilde{q}}$. As a first step we consider the case $A^0 \rightarrow \tilde{q}_1 \tilde{q}_2$ where only F –terms and SUSY breaking terms enter in the coupling. Since A^0 only couples to \tilde{q}_L – \tilde{q}_R and due to the CP nature of A^0 , $A^0 \rightarrow \tilde{q}_i \tilde{q}_i$ vanishes (with real parameters also beyond the tree–level!). Despite the complexity, we have performed the calculation in an analytic way. The explicit formulae will be given elsewhere. We will, however, show the most important results of the numerical analysis. Furthermore, the crossed channel $\tilde{q}_2 \rightarrow \tilde{q}_1 A^0$ is studied.

In case of the decay into sbottom quarks the decay width can receive large corrections which makes the perturbation expansion unreliable, especially for large $\tan \beta$. In some cases the width can even become negative using the on–shell renormalization scheme. We will show that this problem can be fixed by an appropriate choice of the tree–level coupling in terms of $\overline{\text{DR}}$ running quark masses and running A_q .

2 Tree–level result

The squark mixing is described by the squark mass matrix in the left–right basis $(\tilde{q}_L, \tilde{q}_R)$, and in the mass basis $(\tilde{q}_1, \tilde{q}_2)$, $\tilde{q} = \tilde{t}$ or \tilde{b} ,

$$\mathcal{M}_{\tilde{q}}^2 = \begin{pmatrix} m_{\tilde{q}_L}^2 & a_q m_q \\ a_q m_q & m_{\tilde{q}_R}^2 \end{pmatrix} = (R^{\tilde{q}})^\dagger \begin{pmatrix} m_{\tilde{q}_1}^2 & 0 \\ 0 & m_{\tilde{q}_2}^2 \end{pmatrix} R^{\tilde{q}}, \quad (1)$$

where $R_{i\alpha}^{\tilde{q}}$ is a 2×2 rotation matrix with rotation angle $\theta_{\tilde{q}}$, which relates the mass eigenstates \tilde{q}_i , $i = 1, 2$, ($m_{\tilde{q}_1} < m_{\tilde{q}_2}$) to the gauge eigenstates \tilde{q}_α , $\alpha = L, R$, by $\tilde{q}_i = R_{i\alpha}^{\tilde{q}} \tilde{q}_\alpha$ and

$$m_{\tilde{q}_L}^2 = M_Q^2 + (I_q^{3L} - e_q \sin^2 \theta_W) \cos 2\beta m_Z^2 + m_q^2, \quad (2)$$

$$m_{\tilde{q}_R}^2 = M_{\{\tilde{U}, \tilde{D}\}}^2 + e_q \sin^2 \theta_W \cos 2\beta m_z^2 + m_q^2, \quad (3)$$

$$a_q = A_q - \mu (\tan \beta)^{-2I_q^{3L}}. \quad (4)$$

$M_{\tilde{Q}}$, $M_{\tilde{U}}$, and $M_{\tilde{D}}$ are soft SUSY breaking masses, A_q is the trilinear scalar coupling parameter, μ the higgsino mass parameter, $\tan \beta = \frac{v_2}{v_1}$ is the ratio of the vacuum expectation values of the two neutral Higgs doublet states [2, 3], I_q^{3L} denotes the third component of the weak isospin of the quark q , e_q the electric charge in terms of the elementary charge e_0 , and θ_W is the Weinberg angle.

The mass eigenvalues and the mixing angle in terms of primary parameters are

$$m_{\tilde{q}_{1,2}}^2 = \frac{1}{2} \left(m_{\tilde{q}_L}^2 + m_{\tilde{q}_R}^2 \mp \sqrt{(m_{\tilde{q}_L}^2 - m_{\tilde{q}_R}^2)^2 + 4a_q^2 m_q^2} \right) \quad (5)$$

$$\cos \theta_{\tilde{q}} = \frac{-a_q m_q}{\sqrt{(m_{\tilde{q}_L}^2 - m_{\tilde{q}_1}^2)^2 + a_q^2 m_q^2}} \quad (0 \leq \theta_{\tilde{q}} < \pi), \quad (6)$$

and the trilinear breaking parameter A_q can be written as

$$m_q A_q = \frac{1}{2} (m_{\tilde{q}_1}^2 - m_{\tilde{q}_2}^2) \sin 2\theta_{\tilde{q}} + m_q \mu (\tan \beta)^{-2I_q^{3L}}. \quad (7)$$

At tree-level the decay width of $A^0 \rightarrow \tilde{q}_1 \bar{\tilde{q}}_2$ is given by

$$\Gamma^{\text{tree}}(A^0 \rightarrow \tilde{q}_1 \bar{\tilde{q}}_2) = \frac{3 \kappa(m_{A^0}^2, m_{\tilde{q}_1}^2, m_{\tilde{q}_2}^2)}{16 \pi m_{A^0}^3} |G_{123}^{\tilde{q}}|^2 \quad (8)$$

with $\kappa(x, y, z) = \sqrt{(x - y - z)^2 - 4yz}$ and the A^0 - \tilde{q}_i^* - \tilde{q}_j coupling $G_{ij3}^{\tilde{q}}$ given in [6].

3 Full Electroweak Corrections

The one-loop corrected (renormalized) amplitude $G_{123}^{\tilde{q} \text{ ren}}$ can be expressed as

$$G_{123}^{\tilde{q} \text{ ren}} = G_{123}^{\tilde{q}} + \Delta G_{123}^{\tilde{q}} = G_{123}^{\tilde{q}} + \delta G_{123}^{\tilde{q}(v)} + \delta G_{123}^{\tilde{q}(w)} + \delta G_{123}^{\tilde{q}(c)}, \quad (9)$$

where $\delta G_{123}^{\tilde{q}(v)}$ are the vertex corrections (Fig. 1) and $\delta G_{123}^{\tilde{q}(w)}$ the wave-function corrections (Fig. 2). Note that in addition to the one-particle irreducible vertex graphs also one-loop induced reducible graphs with A^0 - Z^0 mixing have to be included. All parameters in the tree-level coupling $G_{123}^{\tilde{q}}$ have to be renormalized due to the shift from the bare to the on-shell values. These corrections are denoted by $\delta G_{123}^{\tilde{q}(c)}$. The full one-loop corrected decay width is then given by

$$\Gamma(A^0 \rightarrow \tilde{q}_1 \bar{\tilde{q}}_2) = \frac{3 \kappa(m_{A^0}^2, m_{\tilde{q}_1}^2, m_{\tilde{q}_2}^2)}{16 \pi m_{A^0}^3} \left[|G_{123}^{\tilde{q}}|^2 + 2\text{Re} \left(G_{123}^{\tilde{q}} \cdot \Delta G_{123}^{\tilde{q}} \right) \right]. \quad (10)$$

Since there are diagrams with photon exchange we also have to consider corrections due to real photon emission to cancel the infrared divergences (Fig. 1). Therefore the corrected (UV- and IR-convergent) decay width is

$$\Gamma^{\text{corr}}(A^0 \rightarrow \tilde{q}_1 \bar{\tilde{q}}_2) \equiv \Gamma(A^0 \rightarrow \tilde{q}_1 \bar{\tilde{q}}_2) + \Gamma(A^0 \rightarrow \tilde{q}_1 \bar{\tilde{q}}_2 \gamma). \quad (11)$$

Throughout the paper we use the SUSY invariant dimensional reduction ($\overline{\text{DR}}$) as regularization scheme. For convenience we perform the calculation in the 't Hooft–Feynman gauge, $\xi = 1$.

3.1 Vertex and wave–function corrections

The relations between the unrenormalized (bare) and renormalized (physical) fields and couplings are

$$\begin{aligned} \mathcal{L}_0 &= \left(G_{123}^{\tilde{q}}\right)^0 \left(A^0\right)^0 \left(\tilde{q}_1^*\right)^0 \left(\tilde{q}_2\right)^0, & \left(G_{123}^{\tilde{q}}\right)^0 &= G_{123}^{\tilde{q}} + \delta G_{123}^{\tilde{q}(c)}, \\ \mathcal{L}^{\text{ren}} &= G_{123}^{\tilde{q}} A^0 \tilde{q}_1^* \tilde{q}_2, & \left(A^0\right)^0 &= \sqrt{1 + \delta Z_{3k}^H} H_k^0, \\ \delta \mathcal{L} &= -\delta G_{123}^{\tilde{q}(v)} A^0 \tilde{q}_1^* \tilde{q}_2, & \left(\tilde{q}_1^*\right)^0 &= \sqrt{1 + \delta Z_{1i}^{\tilde{q}}} \tilde{q}_i^*, \\ & & \left(\tilde{q}_2\right)^0 &= \sqrt{1 + \delta Z_{2j}^{\tilde{q}}} \tilde{q}_j, \end{aligned} \quad (12)$$

with the notation $H_k^0 = \{h^0, H^0, A^0, G^0\}$, $i, j = 1, 2$, and $k = 3, 4$. Thus the renormalized Lagrangian is given by (up to the first order)

$$\mathcal{L}^{\text{ren}} = \left(G_{123}^{\tilde{q}} + \delta G_{123}^{\tilde{q}(v)} + \frac{1}{2} \left(\delta Z_{i1}^{\tilde{q}} G_{i23}^{\tilde{q}} + \delta Z_{j2}^{\tilde{q}} G_{1j3}^{\tilde{q}} + \delta Z_{k3}^H G_{12k}^{\tilde{q}}\right) + \delta G_{123}^{\tilde{q}(c)}\right) A^0 \tilde{q}_1^* \tilde{q}_2. \quad (13)$$

The explicit form of the vertex corrections $\delta G_{123}^{\tilde{q}(v)}$ will be given elsewhere. Due to the antisymmetry of the tree–level coupling, $G_{ij3}^{\tilde{q}} = -G_{ji3}^{\tilde{q}}$, the total wave–function correction reads

$$\delta G_{123}^{\tilde{q}(w)} = \frac{1}{2} \left(\delta Z_{11}^{\tilde{q}} + \delta Z_{22}^{\tilde{q}} + \delta Z_{33}^H\right) G_{123}^{\tilde{q}} + \frac{1}{2} \delta Z_{43}^H G_{124}^{\tilde{q}}. \quad (14)$$

For the wave–function renormalization constants we use the conventional on–shell renormalization conditions [7] which lead to

$$\begin{aligned} \delta Z_{ii}^{\tilde{q}} &= -\Re \dot{\Pi}_{ii}^{\tilde{q}}(m_{\tilde{q}_i}^2), & \delta Z_{43}^H &= \frac{2}{m_{G^0}^2 - m_{A^0}^2} \Re \Pi_{43}^H(m_{A^0}^2), \\ \delta Z_{33}^H &= -\Re \dot{\Pi}_{33}^H(m_{A^0}^2), \end{aligned} \quad (15)$$

with the diagonal parts of the Higgs and squark self–energies $\dot{\Pi}_{ii}(k^2)$.

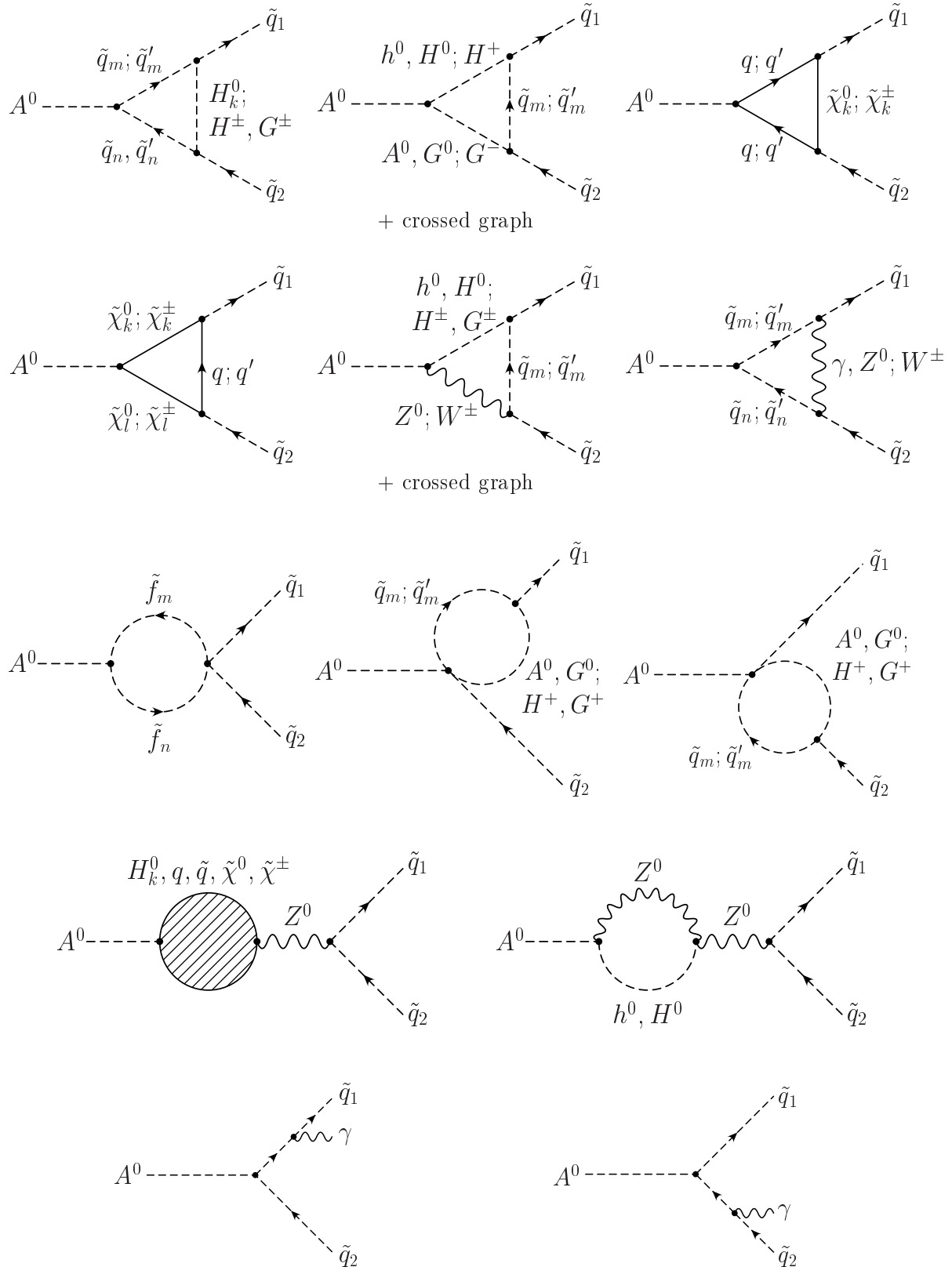


Figure 1: Vertex and photon emission diagrams relevant to the calculation of the virtual electroweak corrections to the decay width $A^0 \rightarrow \tilde{q}_1 \tilde{q}_2$.

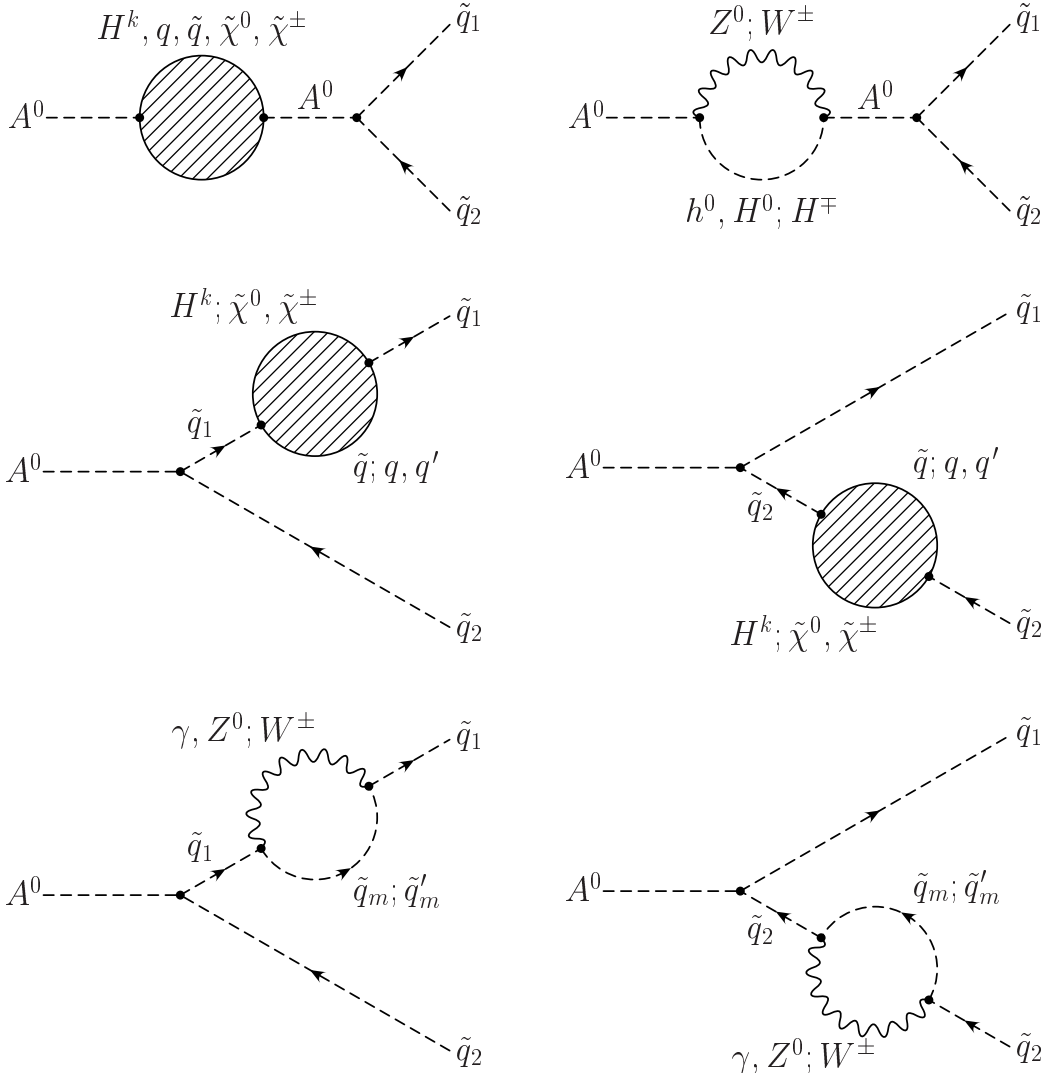


Figure 2: Wave-function diagrams relevant to the calculation of the virtual electroweak corrections to the decay width $A^0 \rightarrow \tilde{q}_1 \tilde{q}_2$. H^k denotes neutral as well as charged Higgs bosons.

The off-diagonal Higgs wave-function corrections can be combined with the contribution to $\delta G_{123}^{\tilde{q}(v)}$ which come from A^0 - Z^0 mixing. First we show that the sum of the parts coming from the propagators of Z^0 and G^0 outside the loops is independent of the gauge parameter $\xi = \xi_Z$.

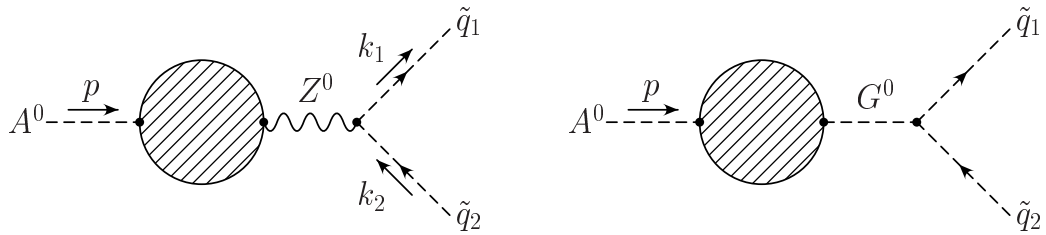


Figure 3: A^0 - Z^0 contribution and A^0 - G^0 wave-function correction

The amplitudes of the two graphs of Fig. 3 in a general R_ξ gauge are

$$\mathcal{M}^Z = \left(-ip^\mu \Pi_{AZ}(p^2) \right) \frac{i}{p^2 - m_Z^2} \left(-g_{\mu\nu} + (1-\xi) \frac{p_\mu p_\nu}{p^2 - \xi m_Z^2} \right) \left(-ig_Z z_{12}^{\tilde{q}} \right) (k_1 + k_2)^\nu, \quad (16)$$

$$\mathcal{M}^G = \left(i \Pi_{AG}(p^2) \right) \frac{i}{p^2 - \xi m_Z^2} i G_{124}^{\tilde{q}}. \quad (17)$$

Contracting the Lorentz indices in \mathcal{M}^Z ,

$$p^\mu \left(-g_{\mu\nu} + (1-\xi) \frac{p_\mu p_\nu}{p^2 - \xi m_Z^2} \right) (k_1 + k_2)^\nu = - \left(1 - \frac{(1-\xi)p^2}{p^2 - \xi m_Z^2} \right) (m_{\tilde{q}_1}^2 - m_{\tilde{q}_2}^2), \quad (18)$$

and eliminating Π_{AG} in favor of Π_{AZ} by using the Slavnov–Taylor identity [8]

$$p^2 \Pi_{AZ}(p^2) + im_Z \Pi_{AG}(p^2) = 0, \quad (19)$$

we find the sum $\mathcal{M}^Z + \mathcal{M}^G$

$$\begin{aligned} \mathcal{M}^{Z+G} &= \frac{i}{p^2 - m_Z^2} \Pi_{AZ}(p^2) g_Z z_{12}^{\tilde{q}} (m_{\tilde{q}_1}^2 - m_{\tilde{q}_2}^2) \left(1 - \frac{(1-\xi)p^2}{p^2 - \xi m_Z^2} \right) \\ &\quad + \frac{p^2}{p^2 - \xi m_Z^2} \frac{\Pi_{AZ}(p^2)}{m_Z} G_{124}^{\tilde{q}}. \end{aligned} \quad (20)$$

Finally we use the identity

$$g_Z z_{ij}^{\tilde{q}} (m_{\tilde{q}_i}^2 - m_{\tilde{q}_j}^2) = im_Z G_{ij4}^{\tilde{q}} \quad (21)$$

to obtain the result

$$\begin{aligned} \delta G_{123}^{\tilde{q}(Z+G)} &= -i \mathcal{M}^{Z+G}(p^2 \rightarrow m_{A^0}^2) = - \frac{i \Pi_{AZ}(m_{A^0}^2) G_{124}^{\tilde{q}}}{m_Z (p^2 - m_Z^2) (p^2 - \xi m_Z^2)} \times \\ &\quad \left[-m_Z^2 \left((p^2 - \xi m_Z^2) - (1-\xi)p^2 \right) + p^2 (p^2 - m_Z^2) \right] \\ &= - \frac{i}{m_Z} \Pi_{AZ}(m_{A^0}^2) G_{124}^{\tilde{q}}. \end{aligned} \quad (22)$$

The gauge dependence of the propagators of the Z^0 and G^0 in Fig. 3 is completely removed. However, there still remain gauge dependences from vector particles and Goldstone bosons in the loops of Π_{AZ} which cancel against their counter parts in the vertex, wave–function and counter term corrections.

3.2 Counter terms

Since all parameters in the tree–level coupling $G_{123}^{\tilde{q}}$ have to be renormalized, we get

$$\delta G_{123}^{\tilde{q}(c)} = \frac{\delta h_q}{h_q} G_{123}^{\tilde{q}} + \frac{i}{\sqrt{2}} h_q \delta \left(A_q \begin{Bmatrix} \cos \beta \\ \sin \beta \end{Bmatrix} + \mu \begin{Bmatrix} \sin \beta \\ \cos \beta \end{Bmatrix} \right) \quad (23)$$

for $\left\{ \begin{array}{c} \text{up} \\ \text{down} \end{array} \right\}$ -type squarks. The Yukawa coupling counter term can be decomposed into corrections to the electroweak coupling g , the masses of the quark q and the gauge boson W and the mixing angle β ,

$$\frac{\delta h_q}{h_q} = \frac{\delta g}{g} + \frac{\delta m_q}{m_q} - \frac{\delta m_W}{m_W} + \left\{ \begin{array}{c} -\cos^2 \beta \\ \sin^2 \beta \end{array} \right\} \frac{\delta \tan \beta}{\tan \beta}. \quad (24)$$

For the trilinear coupling we get with eq. (7)

$$\frac{\delta A_q}{A_q} = \frac{\delta(m_q A_q)}{m_q A_q} - \frac{\delta m_q}{m_q}, \quad (25)$$

$$\begin{aligned} \delta(m_q A_q) &= \delta \left(m_q \mu \left\{ \begin{array}{c} \cot \beta \\ \tan \beta \end{array} \right\} \right) + \frac{1}{2} \left(\delta m_{\tilde{q}_1}^2 - \delta m_{\tilde{q}_2}^2 \right) \sin 2\theta_{\tilde{q}} \\ &\quad + \left(m_{\tilde{q}_1}^2 - m_{\tilde{q}_2}^2 \right) \cos 2\theta_{\tilde{q}} \delta \theta_{\tilde{q}}. \end{aligned} \quad (26)$$

In the on-shell scheme the renormalization condition for the electroweak gauge boson sector reads [9]

$$\frac{\delta g}{g} = \frac{\delta e}{e} + \frac{1}{\tan^2 \theta_W} \left(\frac{\delta m_W}{m_W} - \frac{\delta m_Z}{m_Z} \right) \quad (27)$$

with m_W and m_Z fixed as well as the quark and squark masses as the physical (pole) masses.

Renormalization of the electric charge e

Since we use as input parameter for α the $\overline{\text{MS}}$ value at the Z -pole, $\alpha \equiv \alpha(m_Z)|_{\overline{\text{MS}}} = e^2/(4\pi)$, we get the counter term [10]

$$\begin{aligned} \frac{\delta e}{e} &= \frac{1}{(4\pi)^2} \frac{e^2}{6} \left[4 \sum_f N_C^f e_f^2 \left(\Delta + \log \frac{Q^2}{x_f^2} \right) + \sum_{\tilde{f}} \sum_{m=1}^2 N_C^f e_f^2 \left(\Delta + \log \frac{Q^2}{m_{\tilde{f}_m}^2} \right) \right. \\ &\quad \left. - 4 \sum_{k=1}^2 \left(\Delta + \log \frac{Q^2}{m_{\tilde{\chi}_k^+}^2} \right) - \sum_{k=1}^2 \left(\Delta + \log \frac{Q^2}{m_{H_k^+}^2} \right) - 2 \left(\Delta + \log \frac{Q^2}{m_W^2} \right) \right]. \end{aligned} \quad (28)$$

with $x_f = m_Z \forall m_f < m_Z$ and $x_t = m_t$. N_C^f is the colour factor, $N_C^f = 1, 3$ for (s)leptons and (s)quarks, respectively. Δ denotes the UV divergence factor, $\Delta = 2/\epsilon - \gamma + \log 4\pi$.

Renormalization of $\tan \beta$

For $\tan \beta$ we use the condition [11] $\text{Im} \hat{\Pi}_{A^0 Z^0}(m_A^2) = 0$ which gives the counter term

$$\frac{\delta \tan \beta}{\tan \beta} = \frac{1}{m_Z \sin 2\beta} \text{Im} \Pi_{A^0 Z^0}(m_{A^0}^2). \quad (29)$$

Renormalization of μ

The higgsino mass parameter μ is renormalized in the chargino sector [12, 13] where it enters in the 22–element of the chargino mass matrix X ,

$$X = \begin{pmatrix} M & \sqrt{2}m_w \sin \beta \\ \sqrt{2}m_w \cos \beta & \mu \end{pmatrix} \quad \rightarrow \delta\mu = (\delta X)_{22}. \quad (30)$$

Renormalization of $\theta_{\tilde{q}}$

The counter term of the squark mixing angle, $\delta\theta_{\tilde{q}}$, is fixed such that it cancels the anti–hermitian part of the squark wave–function corrections [14, 15],

$$\delta\theta_{\tilde{q}} = \frac{1}{4} (\delta Z_{12}^{\tilde{q}} - \delta Z_{21}^{\tilde{q}}) = \frac{1}{2(m_{\tilde{q}_1}^2 - m_{\tilde{q}_2}^2)} \text{Re} (\Pi_{12}^{\tilde{q}}(m_{\tilde{q}_2}^2) + \Pi_{21}^{\tilde{q}}(m_{\tilde{q}_1}^2)). \quad (31)$$

3.3 Infrared divergences

The infrared divergences in eq. (10) are cancelled by the inclusion of real photon emission, see the last two Feynman diagrams of Fig. 1. The decay width of $A^0(p) \rightarrow \tilde{q}_1(k_1) + \bar{\tilde{q}}_2(k_2) + \gamma(k_3)$ can be written as

$$\Gamma(A^0 \rightarrow \tilde{q}_1 \bar{\tilde{q}}_2 \gamma) = \frac{3(e e_q)^2 |G_{123}^{\tilde{q}}|^2}{16 \pi^3 m_{A^0}} \left[(m_{A^0}^2 - m_{\tilde{q}_1}^2 - m_{\tilde{q}_2}^2) I_{12} - m_{\tilde{q}_1}^2 I_{11} - m_{\tilde{q}_2}^2 I_{22} - I_1 - I_2 \right] \quad (32)$$

with the phase–space integrals I_n and I_{mn} defined as [16]

$$I_{i_1 \dots i_n} = \frac{1}{\pi^2} \int \frac{d^3 k_1}{2E_1} \frac{d^3 k_2}{2E_2} \frac{d^3 k_3}{2E_3} \delta^4(p - k_1 - k_2 - k_3) \frac{1}{(2k_3 k_{i_1} + \lambda^2) \dots (2k_3 k_{i_n} + \lambda^2)}. \quad (33)$$

The corrected (UV– and IR–convergent) decay width is then given by (see eq. (11))

$$\Gamma^{\text{corr}}(A^0 \rightarrow \tilde{q}_1 \bar{\tilde{q}}_2) \equiv \Gamma(A^0 \rightarrow \tilde{q}_1 \bar{\tilde{q}}_2) + \Gamma(A^0 \rightarrow \tilde{q}_1 \bar{\tilde{q}}_2 \gamma). \quad (34)$$

4 Improvement of One–loop Corrections

In the on–shell renormalization scheme, in case of the decay into sbottom quarks, especially for large $\tan \beta$, the decay width can receive large corrections which makes the perturbation expansion unreliable. In some cases the corrected width can even become negative. It has been pointed out [17, 18] that the source of these large corrections are mainly the counter terms for m_b and the trilinear coupling A_b . We show that this problem can be fixed by absorbing these large counter terms into the A^0 –squark–squark tree–level coupling and expanding the perturbation series around the new tree–level. The technical details will be given in a forthcoming paper.

Correction to m_b

If the Yukawa coupling h_b is given at tree-level in terms of the pole mass m_b , the one-loop corrections to the counter term δm_b become very large due to gluon and gluino exchange contributions. We absorb these large counter terms and also the ones due to loops with electroweak interacting particles into the Higgs–squark–squark tree-level coupling by using the $\overline{\text{DR}}$ running mass $\hat{m}_b(Q=m_A)$. The large counter term due to the gluon loop is absorbed by using SM 2-loop renormalization group equations [18, 19, 20]. Thus we obtain the SM running bottom $\hat{m}_b(Q)_{\text{SM}}$. For large $\tan \beta$ the counter term to m_b can be very large due to the gluino-mediated graph [17, 21, 22]. Here we absorb the gluino contribution as well as the sizeable contributions from neutralino and chargino loops and the remaining electroweak self-energies into the Higgs–squark–squark tree-level coupling. In such a way we obtain the full $\overline{\text{DR}}$ running bottom quark mass

$$\hat{m}_b(Q)_{\text{MSSM}} = \hat{m}_b(Q)_{\text{SM}} + \delta m_b(Q). \quad (35)$$

Correction to A_b

The second source of a very large correction (in the on-shell scheme) is the counter term for the trilinear coupling A_b , eqs. (25, 26), especially the contribution of the left–right mixing elements of the squark mass matrix, $m_{LR}^2 = (m_{\tilde{q}_1}^2 - m_{\tilde{q}_2}^2) \sin \theta_{\tilde{q}} \cos \theta_{\tilde{q}}$. As in the case of the large correction to m_b we use $\overline{\text{DR}}$ running $\hat{A}_b(m_{A^0})$ in the Higgs–squark–squark tree-level coupling. Because of the fact that the counter term δA_b (for large $\tan \beta$) can become several orders of magnitude larger than the on-shell A_b we use $\hat{A}_b(m_{A^0})$ as input [18]. In order to be consistent we have to perform an iteration procedure to get the correct running and on-shell masses, mixing angles and other parameters.

5 Numerical analysis and conclusions

In the following numerical examples, we assume $M_{\tilde{Q}} \equiv M_{\tilde{Q}_3} = \frac{10}{9} M_{\tilde{U}_3} = \frac{10}{11} M_{\tilde{D}_3} = M_{\tilde{L}_3} = M_{\tilde{E}_3} = M_{\tilde{Q}_{1,2}} = M_{\tilde{U}_{1,2}} = M_{\tilde{D}_{1,2}} = M_{\tilde{L}_{1,2}} = M_{\tilde{E}_{1,2}}$ for the first, second and third generation soft SUSY breaking masses and $A \equiv A_t = A_b = A_\tau$, if not stated otherwise. For the standard model parameters we take $m_Z = 91.1876$ GeV, $m_W = 80.423$ GeV, $\sin^2 \theta_W = 1 - m_W^2/m_Z^2$, $\alpha = 1/127.934$, $m_t = 174.3$ GeV, and $m_b = 4.7$ GeV. M' is fixed by the gaugino unification relation $M' = \frac{5}{3} \tan^2 \theta_W M$ and the gluon mass is related to M by $m_{\tilde{g}} = (\alpha_s(m_{\tilde{g}})/\alpha) \sin^2 \theta_W M$.

Decays into stops:

In Fig. 4 we show the tree-level and the corrected width to $A^0 \rightarrow \tilde{t}_1 \tilde{t}_2$ for $\tan \beta = 7$ and $\{M_{\tilde{Q}}, A, M, \mu\} = \{300, -500, 120, -260\}$ GeV as a function of the mass of the decaying Higgs boson, m_{A^0} . As can be seen for larger values of m_{A^0} , the electroweak corrections can be of the same size as the SUSY–QCD corrections.

In Fig. 5 the tree-level, the full electroweak and the full one-loop corrected (electroweak and SUSY–QCD) decay width of $A^0 \rightarrow \tilde{t}_1 \tilde{t}_2$ are given as a function of A_t . The electroweak corrections do not strongly depend on the parameter A_t and are almost constant about 8%. As input parameters we have chosen the values given above as well as

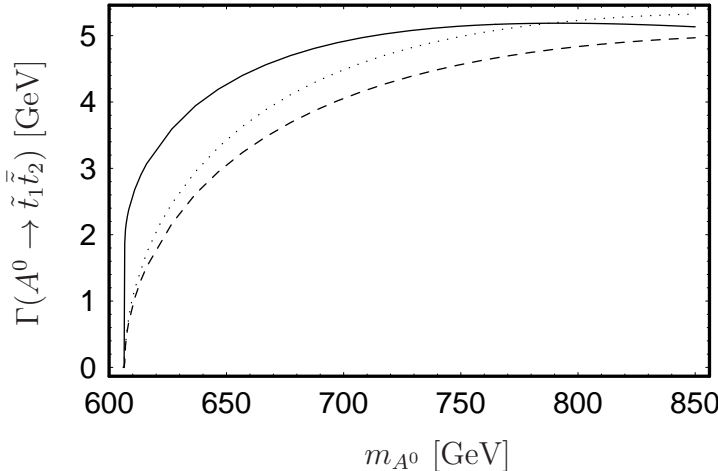


Figure 4: Tree-level (dotted line), full electroweak corrected (dashed line) and full one-loop (electroweak and SUSY-QCD) corrected (solid line) decay width of $A^0 \rightarrow \tilde{t}_1 \tilde{t}_2$.

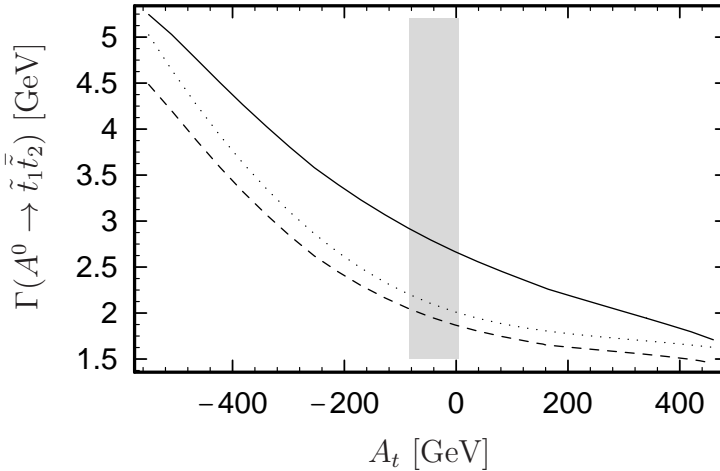


Figure 5: A_t -dependence of tree-level (dotted line), full electroweak corrected (dashed line) and full one-loop (electroweak and SUSY-QCD) corrected (solid line) decay width of $A^0 \rightarrow \tilde{t}_1 \tilde{t}_2$. The gray area is excluded by experimental bounds.

$$\{A_{b,\tau}, m_{A^0}\} = \{-500, 700\} \text{ GeV}.$$

Fig. 6 shows the tree-level, the full electroweak and the full one-loop corrected (electroweak and SUSY-QCD) decay width of $A^0 \rightarrow \tilde{t}_1 \tilde{t}_2$ as a function of $\tan \beta$ with the same parameter set as above and $m_{A^0} = 900$ GeV. Again, in a large region of the parameter space the electroweak corrections are comparable to the SUSY-QCD ones.

Decays into sbottoms:

Here we illustrate the numerical improvement of the full one-loop corrections to $A^0 \rightarrow \tilde{b}_1 \tilde{b}_2$ for large $\tan \beta$.

In Fig. 7 we show two kinds of perturbation expansion for the input parameters $\{m_{A^0}, M_{\tilde{Q}}, A_t, A_b, A_\tau, M, \mu\} = \{800, 300, 150, -700, -500, 120, 260\}$ GeV: First we show

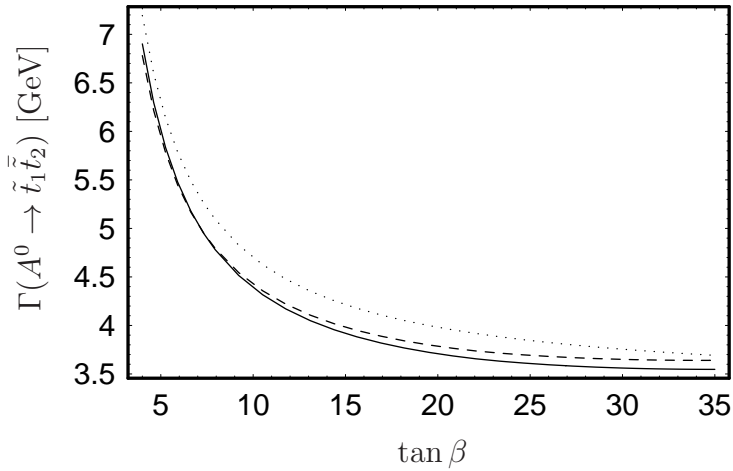


Figure 6: Tree-level (dotted line), full electroweak corrected decay width (dashed line) and full one-loop (electroweak and SUSY-QCD) corrected width (solid line) of $A^0 \rightarrow \tilde{t}_1 \tilde{t}_2$ as a function of $\tan \beta$.

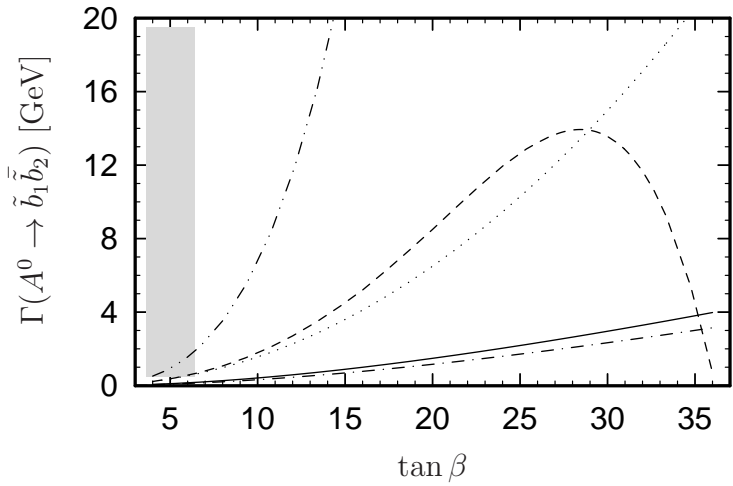


Figure 7: Two kinds of perturbation expansion: the dotted line corresponds to the on-shell tree-level width, the dashed and dash-dot-dotted line correspond to electroweak SUSY-QCD on-shell one-loop width, respectively. The dash-dotted line corresponds to improved the tree-level and the solid line to the (full) improved one-loop width.

the on-shell tree-level width (dotted line). The dashed and dash-dot-dotted line correspond to the on-shell electroweak and full (electroweak plus SUSY-QCD) one-loop width, respectively. For both corrections one can clearly see the invalidity of the on-shell perturbation expansion, in particular the electroweak corrections lead to an improper negative decay width. The second way of perturbation expansion is given by the dash-dotted and the solid line which correspond to the improved tree-level and improved full one-loop decay width, respectively. The smallness of the relative correction in this case shows that the improved tree-level is already a good approximation for $A^0 \rightarrow \tilde{b}_1 \tilde{b}_2$. The input

parameters are the same as in the first case but now with running $A_b = -700$ GeV.

Squarks decays:

Fig. 8 displays the decay widths of the crossed channel $\tilde{t}_2 \rightarrow \tilde{t}_1 A^0$ as a function of A_t . As can be seen, the electroweak corrections are almost twice as large as the SUSY-QCD ones in the considered region. The values of the input parameters are $\{\tan\beta, \mu\} = \{35, -300\}$ and $\{m_{A^0}, m_{\tilde{g}}, M_{\tilde{Q}}, A_b, A_\tau\} = \{150, 1000, 300, -700, -700\}$ GeV with the relations for the SUSY breaking masses given at the top of this section but with $M_{\tilde{U}_3} = 500$ GeV in order to get a quite acceptable mass splitting in the stop sector.

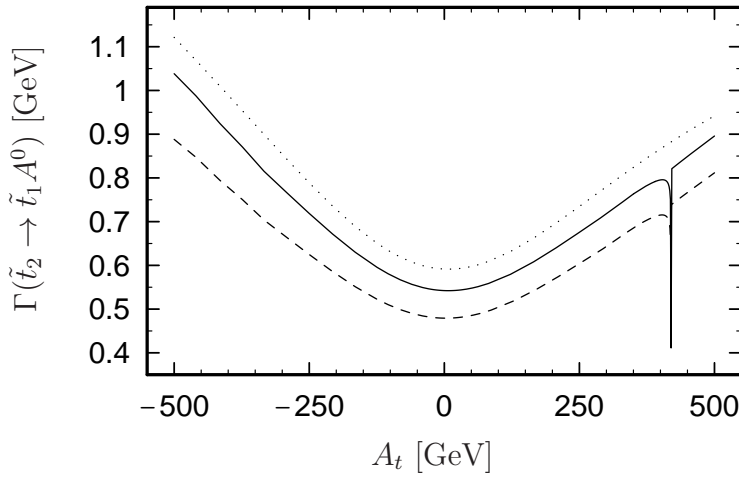


Figure 8: A_t -dependence of the tree-level (dotted line), full electroweak corrected (dashed line) and full one-loop corrected (solid line) decay widths of $\tilde{t}_2 \rightarrow \tilde{t}_1 A^0$.

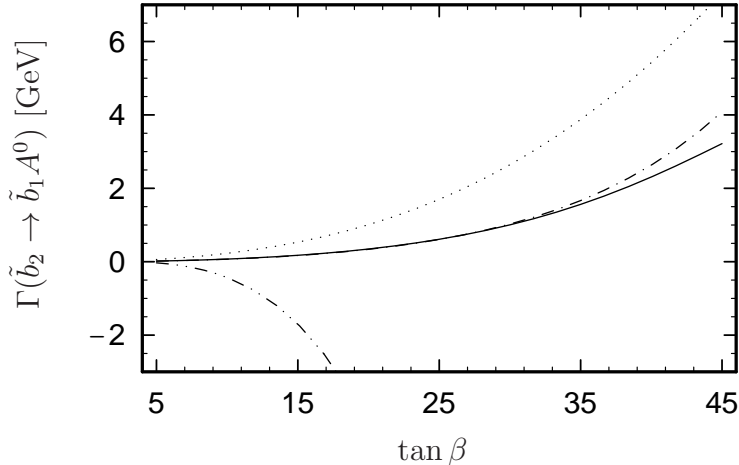


Figure 9: Decay widths of $\tilde{b}_2 \rightarrow \tilde{b}_1 A^0$ as a function of $\tan\beta$. The dotted and dash-dot-dotted line correspond to the on-shell tree-level and on-shell one-loop width, respectively. The dash-dotted line corresponds to the full improved tree-level and the solid line to the full improved one-loop width.

Fig. 9 again demonstrates the numerical improvement in the large $\tan\beta$ regime: The dotted and dash-dot-dotted lines correspond to the on-shell tree-level and on-shell one-loop decay widths of $\tilde{b}_2 \rightarrow \tilde{b}_1 A^0$, whereas the dash-dotted and solid lines show the full improved tree-level and one-loop widths, respectively. The input parameters are the same as in Fig. 8 but with $\{M_{\tilde{Q}_3}, A\} = \{500, -700\}$ GeV.

In conclusion, we have calculated the *full* electroweak one-loop corrections to the decay widths $A^0 \rightarrow \tilde{q}_1 \tilde{q}_2$ and $\tilde{q}_2 \rightarrow \tilde{q}_1 A^0$ in the on-shell scheme. Moreover, we have included the SUSY-QCD corrections which were calculated in [6]. For the decay into sbottom quarks and large $\tan\beta$ an improvement of the on-shell perturbation expansion is necessary. This was done by an appropriate redefinition of the tree-level Higgs-squark-squark coupling. We find that the corrections are significant and in a wide range of the parameter space comparable to the SUSY-QCD corrections.

Acknowledgements

The authors acknowledge support from EU under the HPRN-CT-2000-00149 network programme and the “Fonds zur Förderung der wissenschaftlichen Forschung” of Austria, project No. P13139-PHY.

References

- [1] H. E. Haber and G. L. Kane, Phys. Rep. **117** (1985) 75.
- [2] J. F. Gunion, H. E. Haber, G. L. Kane and S. Dawson, The Higgs Hunter’s Guide, Addison-Wesley (1990).
- [3] J. F. Gunion, H. E. Haber, Nucl. Phys B **272** (1986) 1; B **402** (1993) 567 (E).
- [4] A. Bartl, K. Hidaka, Y. Kizukuri, T. Kon and W. Majerotto, Phys. Lett **315** (1993) 360;
A. Djouadi, J. Kalinowski, P. Ohmann, P.M. Zerwas, Z. Phys. C **74** (1997) 93.
- [5] A. Bartl, H. Eberl, K. Hidaka, T. Kon, W. Majerotto and Y. Yamada, Phys. Lett **378** (1996) 167 and references therein.
- [6] A. Bartl, H. Eberl, K. Hidaka, T. Kon, W. Majerotto and Y. Yamada, Phys. Lett. B **402** (1997) 303;
A. Arhrib, A. Djouadi, W. Hollik, C. Jünger, Phys. Rev. D **57** (1998) 5860.
- [7] M. Böhm, W. Hollik and H. Spiesberger, Fortschr. Phys. **34** (1986) 687.
- [8] A. Dabelstein, Z. Phys. C **67**, 495 (1995); Nucl. Phys. B **456**, 25 (1995).
- [9] A. Sirlin, Phys. Rev. D **22** (1980) 971;
W.J. Marciano and A. Sirlin, Phys. Rev. D **22** (1980) 2695;
A. Sirlin and W.J. Marciano, Nucl. Phys. B **189** (1981) 442.
- [10] H. Eberl, M. Kincel, W. Majerotto and Y. Yamada, Nucl. Phys. B **625** (2002) 372.

- [11] P. H. Chankowski, S. Pokorski, J. Rosiek, Phys. Lett. B **274** (1992) 191; Nucl. Phys. B **423** (1994) 437; 497;
A. Dabelstein, Z. Phys. C **67** (1995) 495; Nucl. Phys. B **456** (1995) 25.
- [12] H. Eberl, M. Kincel, W. Majerotto and Y. Yamada, Phys. Rev. D **64** (2001) 115013.
- [13] W. Öller, H. Eberl, W. Majerotto and C. Weber, hep-ph/0304006, to be published in Eur. Phys. J. C.
- [14] J. Guasch and J. Sola, W. Hollik, Phys. Lett. B **437** (1998) 88.
- [15] H. Eberl, S. Kraml and W. Majerotto, JHEP **9905** (1999) 016.
- [16] A. Denner, Fortschr. Phys. **41** (1993) 307.
- [17] R. Hempfling, Phys. Rev. D **49** (1994) 6168;
L.J. Hall, R. Rattazzi, and U. Sarid, Phys. Rev. D **50** (1994) 7048;
M. Carena, M. Olechowski, S. Pokorski, and C.E.M. Wagner, Nucl. Phys. B **426** (1994) 269;
D.M. Pierce, J.A. Bagger, K. Matchev, and R. Zhang, Nucl. Phys. B **491** (1997) 3.
- [18] H. Eberl, K. Hidaka, S. Kraml, W. Majerotto and Y. Yamada, Phys. Rev. D **62** (2000) 055006.
- [19] E. Braaten and J.P. Leveille, Phys. Rev. D **22** (1980) 715;
M. Drees and K. Hikasa, Phys. Lett. B **240** (1990) 455; **262** (1991) 497 (E);
A. Méndez and A. Pomarol, Phys. Lett. B **252** (1990) 461.
- [20] S.G. Gorishny, A.L. Kataev, S.A. Larin, and L.R. Surguladze, Mod. Phys. Lett. **A5** (1990) 2703; Phys. Rev. D **43** (1991) 1633;
A. Djouadi, M. Spira, and P.M. Zerwas, Z. Phys. C **70** (1996) 427;
A. Djouadi, J. Kalinowski, and M. Spira, Comput. Phys. Commun. **108** (1998) 56;
M. Spira, Fortschr. Phys. **46** (1998) 203.
- [21] M. Carena, S. Mrenna, and C.E.M. Wagner, Phys. Rev. D **60** (1999) 075010; Phys. Rev. D **62** (2000) 055008.
- [22] P.H. Chankowski and S. Pokorski, hep-ph/9707497, in *Perspectives on Supersymmetry*, ed. by G. L. Kane (World Scientific, 1997);
K.S. Babu and C. Kolda, Phys. Lett. B **451** (1999) 77.